JACC: BASIC TO TRANSLATIONAL SCIENCE VOL. 9, NO. 11, 2024

ORIGINAL RESEARCH - LEADING EDGE TRANSLATIONAL RESEARCH

Endothelial Shear Stress Metrics Associate With Proinflammatory Pathways at the Culprit Site of Coronary Erosion

Mona E. Ahmed, MD, PhD,[a,b,c] David M. Leistner, MD,[d,e,f,g,h,i] Diaa Hakim, MD, PhD,[a] Youssef Abdelwahed, MD,[d,e,f] Ahmet U. Coskun, PhD,[j] Charles Maynard, PhD,[k] Claudio Seppelt, MD,[d,e,f,g,i] Gregor Nelles, MD,[d,e,g] Denitsa Meteva, MD,[d,e,f] Nicholas V. Cefalo, BS,[a] Peter Libby, MD,[a] Ulf Landmesser, MD,[d,e,f,g] Peter H. Stone, MD[a]

VISUAL ABSTRACT

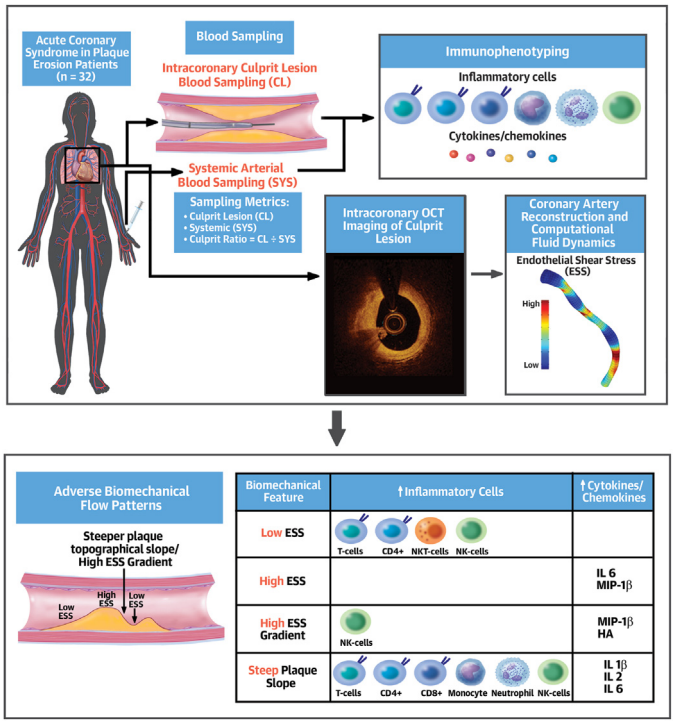

Ahmed ME, et al. JACC Basic Transl Sci. 2024;9(11):1269–1283.

HIGHLIGHTS

- **The pathobiological/pathophysiological mechanisms of atherosclerotic plaque erosion remain largely unexplored.**
- **Proinflammatory local low ESS, high ESSG, and a steep plaque topographical slope are associated with an increased amount of culprit lesion T lymphocytes, $CD4^+$ T lymphocytes, $CD8^+$ lymphocytes as well as natural killer T cells, including their proinflammatory mediators: IL-6, MIP-1β, IL-1β, and IL-2.**
- **This study provides novel mechanistic insights into the relationships between adverse local ESS biomechanical features and the inflammatory microenvironment reflecting different immunomodulatory pathways at the culprit site of plaque erosion.**
- **These findings suggest a possible therapeutic benefit of pre-emptive interventional strategies that ameliorate adverse flow-related biomechanical environments surrounding individual plaques, and thereby prevent future activation of inflammatory pathways responsible for plaque destabilization.**

From the [a]Cardiovascular Division, Brigham and Women's Hospital, Harvard Medical School, Boston, Massachusetts, USA; [b]Department of Molecular Medicine and Surgery, Karolinska Institutet, Stockholm, Sweden; [c]Department of Cardiology, Heart and Vascular Center, Karolinska University Hospital, Stockholm, Sweden; [d]Charité-Universitätsmedizin Berlin, Corporate Member of Freie Universität Berlin and Humboldt-Universität zu Berlin, Berlin, Germany; [e]Deutsches Herzzentrum der Charité, Department of

ISSN 2452-302X https://doi.org/10.1016/j.jacbts.2024.07.008

ABBREVIATIONS AND ACRONYMS

ACS = acute coronary syndrome

CFD = computational fluid dynamics

CL = culprit lesion

CR = culprit lesion ratio

ESS = endothelial shear stress

ESSG = endothelial shear stress gradient

IFC = intact fibrous cap

IFN = interferon

IL = interleukin

IP = interferon-gamma inducible protein

MIP = macrophage inflammatory protein

MLA = minimal lumen area

MMP = matrix metalloproteinase

NF = nuclear factor

NKT = natural killer T (cell)

OCT = optical coherence tomography

SYS = systemic arterial blood

TLR2 = Toll-like receptor 2

SUMMARY

Low endothelial shear stress (ESS) and associated adverse biomechanical features stimulate inflammation, contribute to atherogenesis, and predispose to coronary plaque disruption. The mechanistic links between adverse flow-related hemodynamics and inflammatory mediators implicated in plaque erosion, however, remain little explored. We investigated the relationship of high-risk ESS metrics to culprit lesion proinflammatory/proatherogenic cells and cytokines/chemokines implicated in coronary plaque erosion in patients with acute coronary syndromes. In eroded plaques, low ESS, high ESS gradient, and steepness of plaque topographical slope associated with increased numbers of local T cells and subsets ($CD4^+$, $CD8^+$, natural killer T cells) as well as inflammatory mediators (interleukin [IL]-6, macrophage inflammatory protein-1β, IL-1β, IL-2). (JACC Basic Transl Sci. 2024;9:1269–1283)

Acute coronary syndrome (ACS) remain the main cause of mortality and morbidity worldwide.[1] The ultimate complications of coronary artery disease involve plaque disruption that provokes thrombosis, triggered primarily by plaque rupture or by superficial erosion.[2,3] Erosion, characterized by thrombus formation on a plaque with an intact fibrous cap (IFC) and endothelial injury on the intimal surface, currently accounts for about one-quarter of all ACS events.[4,5] Prior research has implicated inflammatory pathways in the mechanisms of ruptured fibroatheromatous plaque,[2,6] but the pathobiology of plaque erosion has received much less attention. Although lesions underlying sites of erosion generally contain fewer leukocytes than those complicated by rupture, accumulating evidence supports inflammatory processes in endothelial cell injury and the amplification and propagation of thrombosis owing to plaque erosion.[7-11] Previous natural history studies in experimental animals and in humans have identified low endothelial shear stress (ESS) and high endothelial shear stress gradient (ESSG) as proinflammatory and proatherogenic stimuli implicated in coronary plaque development, progression, and destabilization.[12-17] ESSG exerts the strongest effects where the focal ESS is low.[18] Sites of low ESS harbor more inflamed plaques with rupture-prone characteristics, but the relationship of ESS to local immunological characteristics of plaque erosion in humans remains unknown. We previously showed in the OPTICO-ACS (Optical Coherence Tomography in Acute Coronary Syndrome) study that $CD8^+$ T lymphocytes and associated effector molecules, harvested from the culprit lesions in humans, induce endothelial cell injury and apoptosis when incubated with endothelial cells in vitro.[10] Although the role of $CD8^+$ T lymphocytes in the pathogenesis of atherosclerotic plaque formation has undergone extensive investigation,[19,20] few studies have examined the impact of differential hemodynamic and biomechanical conditions on the development of inflammation and plaque destabilization resulting in adverse clinical outcomes. Therefore, this post hoc extension analysis investigated the relationship between the local biomechanical factors and the inflammatory microenvironment at the culprit site of coronary plaque erosion in patients presenting with an ACS.

METHODS

STUDY DESIGN AND PATIENTS. The protocol of the prospective, multicenter OPTICO-ACS study was

Cardiology, Angiology and Intensive Care Medicine, Berlin, Germany; [f]DZHK (German Centre for Cardiovascular Research) partner Site Berlin, Berlin, Germany; [g]DZHK (German Centre for Cardiovascular Research) partner Site Rhine Main, Frankfurt, Germany; [h]Berlin Institute of Health, Berlin, Germany; [i]Department of Cardiology and Angiology, Goethe University, Frankfurt am Main, Germany; [j]Northeastern University, Boston, Massachusetts, USA; and the [k]University of Washington, Seattle, Washington, USA.
Patrick Serruys, MD, served as Guest Associate Editor for this paper. Michael Bristow, MD, PhD, served as Guest Editor-in-Chief for this paper.
The authors attest they are in compliance with human studies committees and animal welfare regulations of the authors' institutions and Food and Drug Administration guidelines, including patient consent where appropriate. For more information, visit the Author Center.

Manuscript received October 31, 2023; revised manuscript received July 16, 2024, accepted July 17, 2024.

previously published.[10] The present post hoc analysis of potential adverse biomechanical triggers of erosion included all 32 patients with optical coherence tomography (OCT)-verified culprit lesions of coronary plaque erosion as the ACS culprit (Supplemental Table 1). Ethical approval was obtained from the Local Ethics Committee (no. EA1/270/16), and the study was conducted in accordance with the Declaration of Helsinki. Written informed consent was obtained from all participating subjects and the study was registered at ClinicalTrials.gov (NCT03129503).

BIOSAMPLE COLLECTION, ANALYSIS, FLOW CYTOMETRY–BASED IMMUNOPHENOTYPING, PLASMA CYTOKINE/CHEMOKINE PROFILING, THROMBUS ANALYSIS. Local culprit lesion (CL) site blood samples, and thrombectomy specimens (aspiration pulled back across the CL), and systemic arterial blood (SYS) samples (radial or femoral artery) were collected and analyzed by flow cytometry-based immunophenotyping and plasma cytokine and chemokine profiling as previously described in detail.[9,10] A brief description of the methodology is also provided in the Supplemental Appendix. The complete array of cytokines, chemokines, and cells analyzed is provided in Supplemental Tables 2 and 3. To investigate CL inflammatory activation, a culprit lesion ratio (CR) was calculated to identify whether the activation pathway in question exhibited a higher concentration at the local CL site compared to a SYS site.

OCT IMAGE ACQUISITION AND ANALYSIS. All OCT images were analyzed in the OPTICO-ACS study for the underlying ACS-causing culprit pathophysiology by 2 independent core labs (Charité Berlin and German Heart Centre Munich) and according to the predefined study-specific standard operating procedure using the Medis QIvus 3.0 (Medis Medical Imaging Service). Details of OCT image acquisition and analysis for defining plaque erosion have been previously published.[10] OCT segmentation was performed at the Vascular Profiling Research Laboratory, Brigham and Women's Hospital, Harvard Medical School. Quantitative and qualitative segmentation was performed using validated offline workstation software, OPTIS ORW E.5.2 (Abbott Vascular, Inc). The luminal area was traced in every frame during the OCT pullback. The minimal lumen area (MLA), measured in square millimeters, which is the smallest lumen area measured in the artery during OCT-pullback; maximum and minimum luminal diameters; reference lumen area; percentage of lumen area stenosis; and thrombus were defined based on previously published expert review documents on OCT methodology, terminology, and clinical applications.[21] Definite erosion was defined as a thrombus overlying a plaque with an IFC, and probable erosion was defined as: 1) luminal endothelial irregularities at the CL site without thrombus; or 2) attenuation of plaque features by an overlying thrombus without superficial lipid or calcified nodules proximal or distal to the thrombus site.[21,22]

CFD CALCULATION. Our methods of intracoronary profiling have been previously described.[23] The 3-dimensional vessel reconstruction, centerline merging, computational fluid dynamics (CFD) simulation, and postprocessing steps were performed according to expert consensus guidelines for patient-specific CFD simulation of blood flow in human coronary arteries.[24] Our CFD methodology is described in detail in the Supplemental Appendix. ESS metrics were calculated along the entire coronary artery and reported in consecutive 3-mm segments in each eroded plaque, which include minimum ESS (Pa/plaque), maximum ESS (Pa/plaque), and maximum ESSG, which is defined as the difference in ESS in immediately adjacent areas of endothelium (Pa/mm), and reported separately as maximum ESSG axial/circumferential plaque upslope/downslope as well as ESSG any direction. We also calculated the plaque topographical slope, defined as the steepness of the plaque either upstream (upslope) or downstream (downslope) from the plaque (Δ lumen area mm^2/frame) for all the eroded plaques. The metric of plaque steepness up- or downslope is a similar metric to the ESSG, measuring the steepness of lumen change, but uses the Δ plaque area per OCT frame instead of CFD-derived ESS changes in immediately adjacent areas.

STATISTICAL ANALYSIS. We analyzed inflammatory markers in CL, SYS, and CR in relation to ESS metrics to capture all possible associations in this exploratory study. Continuous data are presented using the mean ± SD if normally distributed or median (IQR) if skewed. D'Agostino and Pearsons normality test was used to test for normally distributed data. We used both nonparametric and parametric statistical methods. First, in comparing inflammatory markers (immune cells and their effector molecules), as represented by pairs of SYS and CL values, the Wilcoxon signed-rank test was used. Second, to examine the association between the magnitude of shear stress biomechanical metrics and inflammatory activation for select measures of immune cells and cytokines/chemokines, we first examined the association between continuous measures of shear stress

biomechanical metrics and inflammatory activation with the Spearman rank correlation coefficient (*r*). Next, we compared mean values of biomechanical plaque characteristics as continuous variables within categorical tertiles of inflammatory markers with 1-way analysis of variance. *P* value <0.05 was considered statistically significant. Given that this was an exploratory study, we did not adjust *P* values for the many comparisons that were made. Accordingly, we underscore that attention should be paid to the magnitude of differences and not so much to the *P* values. SPSS (version 19.0, IBM Corp) was used for statistical analysis.

RESULTS

BASELINE PATIENT AND PLAQUE CHARACTERISTICS. All 32 plaque erosions from 32 unique patients originally included in the first OPTICO-ACS study[10] analysis proved suitable for OCT segmentation and CFD analysis and constituted the cohort for this substudy. The Visual Abstract shows the study flowchart. Patient demographics including clinical and laboratory data have been previously published (see Supplemental Table 1).

ANATOMICAL AND ESS METRICS. **Table 1** summarizes the baseline plaque characteristics of anatomical and local biomechanical variables obtained from segmented OCT images.

The median MLA was 2.25 (IQR: 1.9) mm^2, the median lumen area stenosis was 63% (IQR: 30%), and the median coronary blood flow was 0.9 (IQR: 0.6) mL/s.

The per plaque median minimum ESS was 1.0 (IQR: 2.4) Pa, the median maximum ESS was 6.9 (IQR: 8.8) Pa, and the median maximum ESSG any direction was 5.4 (IQR: 9.5) Pa/mm. The specific directions of ESSG are displayed in **Table 1**. The median plaque topographical slope up- vs downstream was 1.8 (IQR: 1.5) vs 1.5 (IQR: 1.7) Δ lumen area mm^2/frame, respectively (**Figure 1**).

TOTAL INFLAMMATORY MARKERS DERIVED FROM THE PLAQUE ENVIRONMENT. **Table 2** displays all 41 measured inflammatory markers in the OPTICO-ACS study, including cells, cytokines, and chemokines, both as individual SYS and local CL values, as well as CR values. In general, CL and SYS values of inflammatory markers differed little. Tertiles of these inflammatory cells and biomarkers are summarized in Supplemental Tables 2 and 3. We also noted the CR values in each tertile of inflammatory markers. For the vast majority of inflammatory markers, the CR value in the highest tertile of inflammatory markers was >1.0, indicating an increased elaboration at the culprit site, leading to higher local concentration of the inflammatory marker.

STATISTICAL STRATEGIES TO EVALUATE INFLAMMATORY MARKERS (CELLS, CYTOKINES, AND CHEMOKINES) AND BIOMECHANICAL METRICS. All relationships were compared as 1) "continuous biomechanical variables vs continuous inflammatory variables" as well as 2) "continuous biomechanical variables vs categorical tertiles of inflammatory markers" to capture all potential associations and provide quantitative data on the magnitude of local shear stress.

Inflammatory markers derived from the plaque environment significantly associated with biomechanical metrics. A total of 17 of 41 inflammatory markers (41%) had a statistically significant association with biomechanical metrics/anatomical metrics (**Tables 3 and 4**). We focus our results and discussion on these 17 inflammatory markers (listed in Supplemental Table 4A), which we will describe in detail. Seven (41%) consisted of cells from the adaptive and innate immune system, 10 (59%) consisted of related cytokines/chemokines and extracellular matrix component hyaluronic acid. Five of the 17 inflammatory markers had a numerical CR value >1.0, including T lymphocytes, $CD4^+$ T lymphocytes, intermediate monocytes, and T-cell effector molecules (perforin and granulysin).

Of the 17 inflammatory markers associated with biomechanical metrics, 6 (35%) were associated with multiple biomechanical metrics per inflammatory marker. However, not all inflammatory markers showed statistically significant relationships using statistical approaches that compared biomechanical/anatomical metrics (continuous) with inflammatory markers both as continuous and categorical (tertiles): 4 of 17 inflammatory markers (24%) ($CD8^+$ T lymphocytes, intermediate monocytes, interleukin [IL]-1β, macrophage inflammatory protein [MIP]-1β) displayed statistically significant increased associations with both statistical approaches (continuous vs continuous and continuous vs categorical analyses) (**Tables 3 and 4**), 3 of 17 inflammatory markers (18%) demonstrated statistically significant association with either method, but not both, depending on the biomechanical stimulus (**Tables 3 and 4**). Seven of 17 inflammatory markers (41%) showed statistically significant correlations only for continuous variables of biomechanical/anatomical metrics vs continuous variables of inflammatory markers (**Tables 3 and 4**), and 3 of 17 inflammatory markers (18%) showed statistically significant associations only for continuous

TABLE 1 Plaque Characteristics of the Study Population (N = 32)

MLA, mm^2	2.25 (1.8-3.7)
Area stenosis, %	63 (44.3-74.6)
Blood flow, mL/s	0.9 (0.6-1.2)
Min ESS, Pa	1.0 (0.3-2.7)
Max ESS, Pa	6.9 (2.5-11.3)
Ave ESS, Pa	3.8 (1.8-7.8)
Max ESSG any direction, Pa/mm	5.4 (2.4-11.9)
Max ESSG axial upslope, Pa/mm	3.0 (1.6-6.8)
Max ESSG axial downslope, Pa/mm	5.7 (2.3-11.5)
Max ESSG circumferential upslope, Pa/mm	1.9 (0.9-3.7)
Max ESSG circumferential downslope, Pa/mm	1.5 (0.8-4.3)
Upslope, Δ lumen area mm^2/frame	1.8 (1.2-2.7)
Downslope, Δ lumen area mm^2/frame	1.5 (0.9-2.6)

Values are median (Q1-Q3). Erosion category (definite 19%, probable 81%).
Ave = average; ESS = endothelial shear stress; ESSG = endothelial shear stress gradient; Min = minimum; Max = maximum; MLA = minimal lumen area.

variables of biomechanical metrics vs categorical tertiles of inflammatory markers (Tables 3 and 4).

Inflammatory markers derived from the plaque environment not significantly associated with biomechanical metrics. Twenty-four of 41 examined inflammatory markers (59%) did not display significant associations to adverse shear stress metrics (Supplemental Table 4B), not on a CL, a SYS, nor a CR level, even despite the fact that one-half of these nonassociated inflammatory markers had CR values >1.0 (Table 2), including the following: granzyme A, IL-8, IL-17, MIP-1α, interferon (IFN)-γ, regulated on activation normal T lymphocytes expressed and secreted, matrix metalloproteinase (MMP)-9 activity, tumor necrosis factor-α, granulocyte-macrophage colony-stimulating factor, interferon-gamma inducible protein (IP)-10 and vascular endothelial growth factor, as well as anti-inflammatory IL-10. Of these 12 inflammatory markers that manifested nominally increased concentration at the local CL site, only 7 (58%) had statistically significant increased CR values (granzyme A [$P = 0.021$], MIP-1α [$P = 0.021$], IFN-γ [$P < 0.001$], MMP-9 activity [$P = 0.010$], IL-8 [$P = 0.001$], IL-10 [$P = 0.026$], IP-10 [$P = 0.006$]).

RELATIONSHIP BETWEEN T LYMPHOCYTES AND LOCAL BIOMECHANICAL METRICS. Proinflammatory low minimum ESS associates with T lymphocytes. The relationships between minimum ESS and T lymphocytes are summarized in Table 3. Local minimum ESS correlated inversely with CL T lymphocytes ($r = -0.381$, $P = 0.038$) as well as CL and SYS values of natural killer T (NKT) cells ($r = -0.366$, $P = 0.047$; $r = -0.374$, $P = 0.042$, respectively) in eroded plaques. The same numerical trend pertained to the lowest mean values of minimum ESS that was found in the highest tertile of CL T lymphocytes and NKT cells (1.0 ± 0.96 Pa and 0.93 ± 0.127 Pa, respectively), although these findings were not statistically significant ($P = 0.38$ and $P = 0.32$, respectively). In addition, the lowest mean value of minimum ESS was also observed in the highest tertile of CL $CD4^+$ T lymphocytes (1.0 ± 0.96 Pa, $P = 0.046$).

The magnitude of plaque topographical upslope associates with T lymphocytes. The relationships between plaque topographical slope and T lymphocytes are summarized in Table 3. A steeper plaque topographical upslope correlated positively with CL and SYS values of T lymphocytes ($r = 0.439$, $P = 0.015$; $r = 0.422$, $P = 0.020$, respectively), $CD4^+$ T lymphocytes ($r = 0.455$, $P = 0.012$; $r = 0.456$, $P = 0.011$, respectively) and $CD8^+$ T lymphocytes ($r = 0.483$, $P = 0.007$; $r = 0.443$, $P = 0.014$, respectively). The relationship between plaque upslope and $CD8^+$ T lymphocytes was internally consistent showing statistically significant results with the 2 statistical methods. The steepest plaque upslope was found in the highest tertile of CL $CD8^+$ T lymphocytes (2.7 ± 1.4 Δ lumen area mm^2/frame, $P = 0.008$). Although not statistically significant, the categorical data followed the same trend and displayed the steepest plaque topographical upslope in the highest tertile of CL T lymphocytes, and $CD4^+$ T lymphocytes (2.9 ± 1.3 Δ lumen area mm^2/frame, $P = 0.17$; and $P = 0.20$, respectively).

RELATIONSHIP BETWEEN INNATE IMMUNE CELLS AND LOCAL BIOMECHANICAL METRICS. The relationships between innate immune cells and local biomechanical metrics are summarized in Table 3. We found an increased number of NK cells associated with several adverse biomechanical metrics, including low minimum ESS, high ESSG axial upslope, and a steeper plaque topographical upslope at the CL site. The lowest mean value of proinflammatory minimum ESS was observed in the highest tertile of CR of NK cells (0.8 ± 0.78 Pa, $P = 0.041$). The magnitude of plaque topographical upslope was positively correlated with CL and SYS NK cells ($r = 0.388$, $P = 0.034$; $r = 0.378$, $P = 0.040$, respectively). The highest mean value of maximum ESSG axial upslope associated with the highest tertile of CL NK cells (7.7 ± 6.7 Pa/mm, $P = 0.043$). Despite observing a significantly lower values of neutrophils and granulocytes at the culprit lesion site as compared to the systemic site (CR: 0.89, $P < 0.001$) we found a significant association to plaque topographical downslope. The steepest mean plaque downslope was observed in the highest tertile of CL

FIGURE 1 Relationship Between Local Adverse Plaque Biomechanics and Inflammatory Mediators

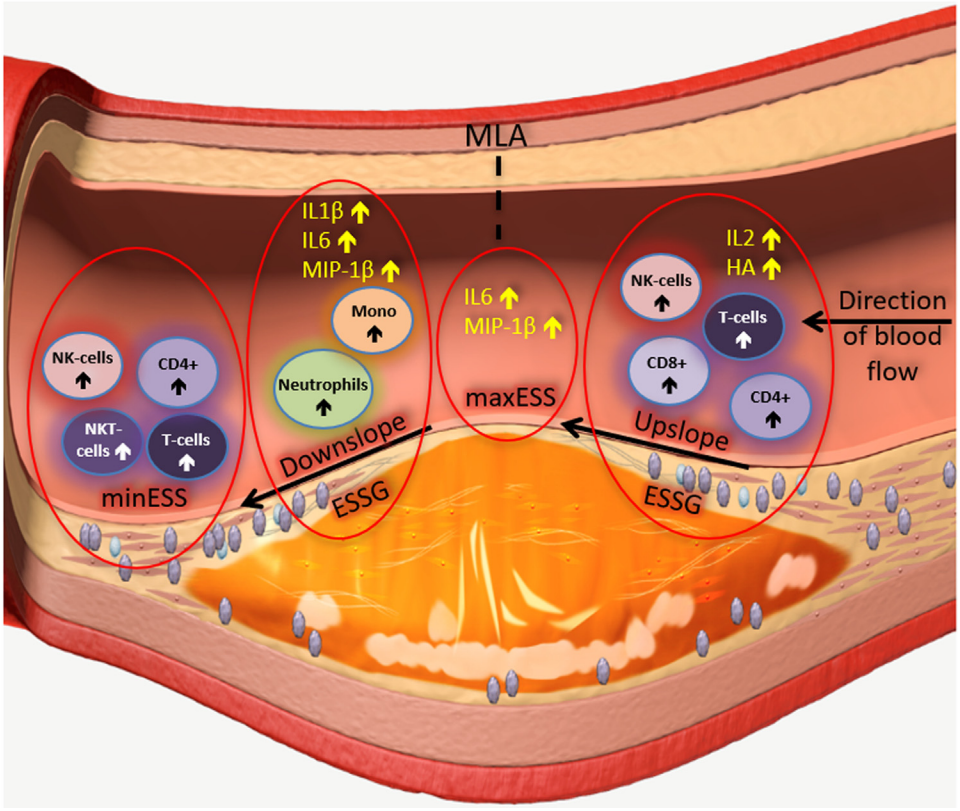

Schematic drawing showing the proposed mechanisms involved in the pathobiology of coronary plaque erosion. Flow-related hemodynamics modify local shear stress patterns on the endothelial monolayer and trigger inflammatory processes. $CD4^+$ = CD4+ T cells; ESSG = endothelial shear stress gradient; HA = hyaluronic acid; IL = interleukin; maxESS = maximum endothelial shear stress; minESS = minimum endothelial shear stress; MIP = macrophage inflammatory protein; MLA = minimal lumen area; Mono = monocyte; NK = natural killer; NKT = natural killer T (cells); T cells = T lymphocytes.

neutrophils, as well as CL and SYS intermediate monocytes (2.7 ± 1.3 Δ lumen area mm^2/frame, $P = 0.046$; 2.8 ± 1.7 Δ lumen area mm^2/frame, $P = 0.012$; 2.7 ± 1.57 Δ lumen area mm^2/frame, $P = 0.039$, respectively). A steeper plaque downslope was also positively correlated to CL and SYS intermediate monocytes ($r = 0.490$, $P = 0.006$; $r = 0.524$, $P = 0.003$, respectively).

RELATIONSHIP BETWEEN T LYMPHOCYTE–RELATED CYTOKINES/CHEMOKINES AND LOCAL BIOMECHANICAL METRICS. Innate immune cells play a critical role in activation and differentiation of T lymphocytes through the production of different proinflammatory cytokines and vice versa. Some of the most important proinflammatory cytokines responsible for T-lymphocyte activation and differentiation associated with specific biomechanical metrics.

Interleukins. The relationships between interleukins and local biomechanical metrics are summarized in Table 4. The magnitude of plaque topographical downslope was positively correlated with CR of IL-1β and IL-6 ($r = 0.499$, $P = 0.005$; and $r = 0.706$, $P = 0.015$, respectively). The steepest plaque downslope was observed in the highest tertile of CR of IL-1β (2.8 ± 1.6 Δ lumen area mm^2/frame, $P = 0.017$). Furthermore, the steepest plaque topographical downslope was found in the highest tertile of CR IL-6, but the comparisons were not statistically significant (2.4 ± 1.5 Δ lumen area mm^2/frame, $P = 0.099$). In addition, local maximum ESS at the site of the MLA was also positively correlated with CR of IL-6 ($r = 0.609$, $P = 0.047$). In regard to anatomical metrics, the smallest MLA and the highest percentage of luminal area stenosis was observed in the highest

TABLE 2 Culprit Lesion and Systematic Inflammatory Biomarkers (N = 32)

Inflammatory Markers	Culprit Lesion	Systemic	Culprit Ratio	*P* Value
Immune cells				
T lymphocytes, absolute	3,509 (1,963-5,397)	3,596 (1,596-5,868)	1.01 (0.93-1.15)	0.81
$CD4^+$ T cells, absolute	1,880 (1,372-3,679)	2,113 (1,239-3,973)	1.03 (0.94-1.12)	0.78
$CD8^+$ T cells, absolute	838 (478-1,585)	847 (394-1,741)	0.99 (0.87-1.20)	0.51
NKT cells, absolute	45 (23-69)	45 (19-69)	0.94 (0.81-1.29)	0.91
B cells, absolute	1,088 (476-1,636)	1,308 (506-1,831)	0.95 (0.84-1.08)	0.032
Total monocytes, absolute	2,265 (1,727-3,440)	2,323 (1,723-4,142)	0.96 (0.83-1.06)	0.051
Classical monocytes, absolute	2,180 (1,539-3,256)	2,186 (1,665-3,701)	0.95 (0.82-1.05)	0.049
Intermediate monocytes, absolute	41 (22-69)	45 (25-76)	1.11 (0.81-1.34)	0.91
Alternative monocytes, absolute	63 (41-140)	82 (47-133)	0.97 (0.82-1.23)	0.23
Granulocytes, absolute	40,496 (27,905-60,910)	44,775 (35,648-68,558)	0.89 (0.77-1.01)	<0.001
Neutrophils, absolute	35,052 (25,723-55,576)	37,386 (30,611-61,152)	0.89 (0.76-1.01)	<0.001
NK cells, absolute	1,314 (853-2,661)	1,395 (812-3,061)	0.97 (0.83-1.15)	0.28
Cytokines and chemokines				
IL-1β, pg/mL	10.34 (6.33-18.26)	11.42 (6.63-16.86)	1.00 (0.78-1.44)	0.64
IL-2, pg/mL	11.20 (11.20-12.14)	11.20 (11.20-12.60)	1.00 (0.96-1.00)	0.69
IL-3, pg/mL	2.71 (1.86-4.56)	3.79 (1.86-5.28)	0.87 (0.60-1.44)	0.72
IL-4, pg/mL	1.40 (1.40-1.82)	1.40 (1.40-1.78)	1.00 (0.79-1.74)	0.92
IL-5, pg/mL	1.10 (1.10-1.10)	1.10 (1.10-1.10)	1.00 (1.00-1.00)	0.99
IL-6, pg/mL	10.24 (5.88-12.57)	6.23 (5.22-14.33)	1.00 (0.67-1.70)	0.88
IL-8, pg/mL	8.82 (6.49-12.46)	7.00 (4.30-10.24)	1.20 (1.06-1.67)	0.001
IL-10, pg/mL	3.16 (2.20-5.01)	2.59 (1.82-4.04)	1.12 (0.94-1.42)	0.026
IL-13, pg/mL	4.70 (3.65-5.52)	4.64 (3.04-5.61)	1.00 (0.93-1.26)	0.58
IL-17, pg/mL	18.11 (14.77-22.47)	15.11 (12.8-19.85)	1.20 (0.93-1.43)	0.13
GM-CSF, pg/mL	2.78 (2.09-3.11)	2.55 (2.22-2.83)	1.18 (0.81-1.25)	0.33
INF-γ, pg/mL	12.45 (10.28-15.91)	10.95 (8.64-13.74)	1.13 (1.02-1.28)	<0.001
IP-10, pg/mL	435.7 (316-575.9)	317.1 (222.0-527.8	1.32 (1.02-1.63)	0.006
MCP-1, pg/mL	55.85 (36.01-88.93)	64.38 (34.73-130.6)	0.90 (0.57-1.13)	0.021
MIP-1α, pg/mL	2.19 (1.78-3.51)	1.56 (1.25-1.75)	1.59 (1.11-2.09)	0.021
MIP-1β, pg/mL	13.93 (9.58-21.94)	18.55 (10.86-25.32)	0.85 (0.69-1.05)	0.024
RANTES, pg/mL	2,691 (1,366-3,104)	1,991 (1,840-2,360)	1.19 (0.84-1.44)	0.16
CD40 ligand, pg/mL	186 (103.9-230.8)	162.2 (118.4-253.4)	0.82 (0.59-1.60)	0.72
TNF-α, pg/mL	4.92 (3.28-7.86)	4.92 (3.74-8.29)	1.01 (0.79-1.27)	0.99
VEGF, pg/mL	6.77 (4.50-9.73)	6.20 (4.50-7.10)	1.15 (0.92-1.49)	0.26
TGF-β, ng/mL	14.90 (14.90-14.90)	14.90 (14.90-14.90)	1.00 (1.00-1.00)	0.32
bFGF, pg/mL	28.61 (21.55-36.84)	29.86 (21.40-40.05)	0.98 (0.80-1.08)	0.093
Granzyme A, pg/mL	11.01 (8.30-13.27)	7.72 (5.77-10.03)	1.47 (0.98-1.93)	0.021
Perforin, pg/mL	1,982 (894.1-4,083)	1,801 (71.14-2,795)	1.81 (0.84-41.31)	0.16
Granulysin, pg/mL	6,369 (1,043-15,006)	3,784 (261.3-8,455)	1.91 (0.87-3.99)	0.33
NGAL, ng/mL	591.1 (349.4-666.4)	745.6 (428.3-982.5)	0.79 (0.70-0.93)	<0.001
Hyaluronic acid, ng/mL	70.31 (29.84-187)	84.71 (49.58-232.5)	0.79 (0.54-0.94)	0.004
MMP-9, ng/mL	70.63 (45.08-130.8)	81.93 (52.47-122.5)	0.93 (0.64-1.33)	0.72
MMP-9 activity, u/μL	0.08 (0.08-0.46)	0.08 (0.08-0.40)	1.03 (0.98-1.16)	0.010

Values are median (Q1-Q3). Culprit lesion ratio = local level culprit lesion site/systemic level arterial sheath). Unit of measurements (absolute cell count [absolute] / 10 μL of whole blood, plasma concentration: pg/mL, ng/mL, u/μL).

bFGF = basic fibroblast growth factor; GM-CSF = granulocyte-macrophage colony-stimulating factor; IFN = interferon gamma; IL = interleukin; IP = interferon gamma-inducible protein; MCP = monocyte chemoattractant protein; MIP = macrophage inflammatory protein; MMP = matrix metallopeptidase; NGAL = neutrophil gelatinase-associated lipocalin; NK = natural killer; NKT = natural killer T (cells); RANTES = regulated on activation normal T lymphocytes expressed and secreted, T cells = T lymphocytes; TGF = transforming growth factor; TNF = tumor necrosis factor; VEGF = vascular endothelial growth factor.

tertile of CR IL-6 (1.96 ± 0.3 mm^2, $P = 0.002$ and $72 \pm 11\%$, $P = 0.017$, respectively). Finally, the magnitude of plaque topographical upslope was positively correlated with CL IL-2 ($r = 0.649$, $P = 0.031$).

Chemotactic cytokines. The relationships between chemokines and local biomechanical metrics are summarized in Table 4. Several adverse biomechanical metrics associated with a higher local concentration of MIP-1β. Local maximum ESS at the site of the MLA correlated positively with local concentration of MIP-1β ($r = 0.402$, $P = 0.034$), and the highest mean value of local maximum ESS was observed in

TABLE 3 Proinflammatory Adverse Outcomes in Relation to Anatomical and Biomechanical Metrics

Immune Cells	Biomechanical Metric and Anatomical Variables	Correlation[a] (*r*, *P* Value)	Tertiles[b] (Mean ± SD, *P* Value)	Comments
Culprit lesion				
T-cells	Min ESS	−0.381, 0.038	1.0 ± 0.96, 0.38	Inverse correlation indicating that a lower mean min ESS is associated with a higher T-cell count (tertile 3)
	Plaque upslope	0.439, 0.015	2.9 ± 1.3, 0.17	Positive correlation indicating that a steeper mean upslope is associated with a higher T-cell count (tertile 3)
$CD4^+$ T cells	Min ESS	−0.342, 0.064	1.0 ± 0.96, 0.046	Inverse correlation indicating that a lower mean min ESS is associated with a higher $CD4^+$ T-cell count (tertile 3)
	Plaque upslope	0.455, 0.012	2.9 ± 1.3, 0.20	Positive correlation indicating that a steeper mean upslope is associated with a higher $CD4^+$ T-cell count (tertile 3)
$CD8^+$ T cells	Plaque upslope	0.483, 0.007	2.7 ± 1.4, 0.008	Positive correlation indicating that a steeper mean upslope is associated with a higher $CD8^+$ T-cell count (tertile 3)
NKT cells	Min ESS	−0.366, 0.047	0.93 ± 0.127, 0.32	Inverse correlation indicating that a lower mean min ESS is associated with a higher NKT-cell count (tertile 3)
NK cells	Max ESSG axial upslope	0.194, 0.35	7.7 ± 6.7, 0.043	A higher mean max ESSG axial upslope is associated with a higher NK-cell count (tertile 3)
	Plaque upslope	0.388, 0.034	2.9 ± 1.3, 0.17	Positive correlation indicating that a steeper mean upslope is associated with a higher NK-cell count (tertile 3)
Intermediate monocytes	Plaque downslope	0.490, 0.006	2.8 ± 1.7, 0.012	Positive correlation indicating that a steeper mean downslope is associated with a higher intermediate monocyte cell count (tertile 3)
Neutrophils	Plaque downslope	0.005, 0.98	2.7 ± 1.3, 0.046	A steeper mean downslope is associated with a higher neutrophil cell count (tertiles 2 and 3)
Systemic values				
T cells	Plaque upslope	0.422, 0.020	2.8 ± 1.3, 0.19	Positive correlation, indicating that a steeper mean upslope is associated with a higher T-cell count (tertile 3)
$CD4^+$ T cells	Plaque upslope	0.456, 0.011	2.6 ± 1.1, 0.17	Positive correlation, indicating that a steeper mean upslope is associated with a higher $CD4^+$ T-cell count (tertile 3)
$CD8^+$ T cells	Plaque upslope	0.443, 0.014	2.7 ± 1.4, 0.077	Positive correlation, indicating that a steeper mean upslope is associated with a higher $CD8^+$ T-cell count (tertile 3)
NKT cells	Min ESS	−0.374, 0.042	1.0 ± 1.3, 0.26	Inverse correlation indicating that a lower mean min ESS is associated with a higher NKT-cell count (tertile 3)
NK cells	Plaque upslope	0.378, 0.040	2.6 ± 1.2, 0.26	Positive correlation, indicating that a steeper mean upslope is associated with a higher NK-cell count (tertile 3)
Intermediate monocytes	Plaque downslope	0.524, 0.003	2.7 ± 1.57, 0.039	Positive correlation, indicating that a steeper mean downslope is associated with a higher Intermediate monocyte cell count (tertile 3)
Culprit ratio				
NK cells	Min ESS	−0.148, 0.43	0.8 ± 0.78, 0.041	A lower mean min ESS is associated with a higher NK-cell count (tertile 3)

Tertiles: 1-3 = low to high. Inflammatory cells: N = 32. [a]Correlation represents continuous biomechanical vs inflammatory markers. [b]Tertiles represent continuous biomechanical vs categorical tertiles of inflammatory markers.

Abbreviations as in Tables 1 and 2.

the highest tertile of CL MIP-1β (11.1 ± 6.2 Pa, $P = 0.056$). In addition, ESSG was also associated with increased levels of MIP-1β. Both maximum ESSG axial upslope and maximum ESSG circumferential downslope correlated positively with CL MIP-1β ($r = 0.473$, $P = 0.020$; and $r = 0.538$, $P = 0.007$, respectively). The maximum ESSG circumferential downslope also positively correlated with the systemic value of MIP-1β ($r = 0.560$, $P = 0.003$). Furthermore, the highest mean value of maximum ESSG axial upslope and maximum ESSG circumferential downslope were found in the highest tertile of MIP-1β (6.8 ± 5.7 Pa/mm, $P = 0.11$; and 5.2 ± 3.6 Pa/mm, $P = 0.016$, respectively).

T-cell effector molecules. A smaller MLA correlated with an increased CR of T-cell effector molecules: Perforin ($r = -0.809$, $P = 0.003$) and granulysin ($r = -0.645$, $P = 0.032$). A higher maximum ESSG axial upslope was associated with a higher concentration of hyaluronic acid at the CL site (9.5 ± 6.6 Pa/mm, $P = 0.016$) (Table 4).

ATHEROPROTECTIVE ANTI-INFLAMMATORY MEDIATORS AND ADVERSE BIOMECHANICAL METRICS. Among the putative atheroprotective inflammatory mediators (IL-4, IL-10, IL-13, and transforming growth factor-β) we observed a statistically significant suppression of systemic IL-4 in relation to a steeper plaque upslope and a higher maximum ESSG axial upslope

TABLE 4 Proinflammatory Adverse Outcomes in Relation to Anatomical and Biomechanical Metrics

Cytokines and Chemokines	Biomechanical Metric and Anatomical Variables	Correlation[a] (*r*, *P* Value)	Tertiles[b] (Mean ± SD, P Value)	Comments
Culprit lesion				
IL-2	Plaque upslope	0.649, 0.031	2.1 ± 1.8, 0.23	Positive correlation indicating that a steeper mean upslope is associated with a higher concentration of IL-2 (tertile 3)
MIP-1β	Max ESS	0.402, 0.034	11.1 ± 6.2, 0.056	Positive correlation indicating that a higher mean max ESS is associated with a higher concentration of MIP-1β (tertile 3)
	Ave ESS	0.384, 0.044	7.4 ± 5.3, 0.68	Positive correlation indicating that a higher mean ave ESS is associated with a higher concentration. of MIP-1β (tertile 3)
	Max ESSG axial upslope	0.473, 0.020	6.8 ± 5.7, 0.11	Positive correlation indicating that a higher mean max ESSG axial upslope is associated with a higher concentration of MIP-1β (tertile 3)
	Max ESSG circumferential downslope	0.538, 0.007	5.2 ± 3.6, 0.016	Positive correlation indicating that a higher mean max ESSG circumferential downslope is associated with a higher concentration of MIP-1β (tertile 3)
Hyaluronic acid	Max ESSG axial upslope	0.365, 0.17	9.5 ± 6.6, 0.016	A higher mean max ESSG axial upslope is associated with a higher concentration of hyaluronic acid (tertiles 2 and 3)
Systemic values				
MIP-1β	Max ESSG circumferential downslope	0.560, 0.003	0.68 ± 0.49, 0.24	Positive correlation, indicating that a higher mean max ESSG circumferential downslope is associated with a higher concentration of MIP-1β (tertile 3)
IL-4 (atheroprotective)	Max ESSG axial upslope	−0.753, 0.019	4.5 ± 3.2, 0.15	Inverse correlation indicating that a higher mean max ESSG axial upslope is associated with a lower concentration of IL4 (tertile 1)
	Plaque upslope	−0.670, 0.024	2.7 ± 2.1, 0.13	Inverse correlation indicating that a steeper mean upslope is associated with a lower concentration of IL-4 (tertile 1)
Culprit ratio				
IL-1β	Plaque downslope	0.499, 0.005	2.8 ± 1.6, 0.017	Positive correlation indicating that a steeper mean downslope is associated with a higher concentration of IL-1β (tertile 3)
IL-3	Max ESSG circumferential downslope	0.800, 0.010	3.4 ± 2.2, 0.15	Positive correlation indicating that a higher mean max ESSG circumferential downslope is associated with a higher concentration of IL-3 (tertile 3)
IL-6	Max ESS	0.609, 0.047	9.0 ± 4.2, 0.064	Positive correlation indicating that a higher mean max ESS is associated with a higher concentration of IL-6 (tertile 3)
	Plaque downslope	0.706, 0.015	2.4 ± 1.5, 0.099	Positive correlation indicating that a steeper mean downslope is associated with a higher concentration of IL-6 (tertile 3)
	MLA, mm^2	−0.418, 0.20	1.96 ± 0.3, 0.002	A smaller MLA is associated with a higher concentration of IL-6 (tertile 3)
	Area stenosis, %	0.600, 0.051	72 ± 11, 0.017	A bigger area stenosis is associated with a higher concentration of IL-6 (tertile 3)
Granulysin	MLA, mm^2	−0.645, 0.032	1.6 ± 0.1, 0.16	A smaller MLA correlates with a higher concentration of granulysin (tertile 3)
Perforin	MLA, mm^2	−0.809, 0.003	1.6 ± 0.1, 0.17	A smaller MLA correlates with a higher concentration of perforin (tertile 3)
bFGF	Plaque downslope	0.230, 0.22	2.7 ± 1.8, 0.029	A steeper mean downslope is associated with a higher concentration of bFGF (tertile 3)

Cytokines and chemokines: n = 32. Tertiles: 1-3 = low to high. [a]Correlation represents continuous biomechanical vs inflammatory markers. [b]Tertiles represent continuous biomechanical vs categorical tertiles of inflammatory markers.

Abbreviations as in Tables 1 and 2.

($r = -0.670$, $P = 0.024$; and $r = -0.753$, $P = 0.019$, respectively). Inflammatory messengers with pro- or anti-inflammatory features, including IP-10, neutrophil gelatinase-associated lipocalin, and granulocyte-macrophage colony-stimulating factor, did not display an association with adverse biomechanical metrics.

DISCUSSION

This study investigated the detailed relationships between the local ESS and topographical biomechanical factors and the inflammatory microenvironment reflecting different immunomodulatory pathways at the culprit site of coronary plaque

erosion in patients with an ACS (**Figure 1**). Our main findings were the following:

1. Adaptive immune responses: A lower local minimum ESS and a steeper plaque topographical slope were associated with increased CL T lymphocytes, including subsets of T lymphocytes ($CD4^+$, $CD8^+$, and NKT cells) in eroded plaques.
2. Innate immune responses: A lower local minimum ESS and a steeper plaque topographical slope were associated with increased CL innate immune cells such as NK cells and neutrophils.
3. Proinflammatory cytokine responses: Local adverse ESS metrics such as high maximum ESS, high ESSG, and a steeper plaque topographical slope associated with T lymphocyte–related proinflammatory cytokines/chemokines (ie, IL-6, MIP-1β, IL-1β, and IL-2) at the CL site.

DIFFERENT MAGNITUDES OF ESS BIOMECHANICAL METRICS TRIGGER DIFFERENT VASCULAR RESPONSES IN PLAQUE EROSION. ESS values along the course of an individual plaque influence the endothelium and drive either local vasculoprotective or inflammatory responses, based on the nature and magnitude of the ESS stimulus.[12] Local adverse ESS stimuli trigger inflammatory responses, which may initiate a cascade of events that results in degradation of the basement membrane and endothelial cell desquamation and death leading to intimal erosion and thrombus formation.[25] Indeed, human data have recently affirmed the clinical relevance of our previous mechanistic experimental studies in this regard.[9]

Low ESS (<1.3 Pa) is a proinflammatory and proatherogenic stimulus, resulting in atheroprogressive gene expression and activation of a variety of inflammatory cellular and molecular responses in endothelial cells[12,26-29] and as evidenced by its independent role in plaque destabilization and precipitation of major adverse clinical events in humans with coronary artery disease.[15,16]

Different magnitudes of high ESS (>~2.5 Pa) may be associated with very different vascular responses, although the absolute levels of high ESS responsible for the different pathobiologic responses have not been clearly identified. Mild to moderate elevations of high ESS from experimentally induced increased focal arterial flow, for example, exert a vasculoprotective effect of outward vascular remodeling, a potential adaptive response to restore physiologic ESS levels (~1.3-2.5 Pa) in that area.[30] In contrast, very high ESS values, up to 20-fold higher than physiologic ESS, may lead to endothelial cell injury and may be associated with plaque disruption and major adverse clinical events.[31-33]

High ESS most likely exerts its pathobiological effect in a setting of an immediately adjacent low ESS environment (ie, high ESSG), which commonly occurs up- or downstream from a substantial luminal obstruction.[18] The ESSG can be in any spatial direction, such as axial, circumferential, or up- or downslope of the topographical plaque obstruction. More recent findings have identified ESSG as a more adverse pathobiologic metric than either high or low ESS alone.[17] Prior studies reinforce the notion of the effect of ESSG and different directions of ESSG on gene expression[27,34] and cell loss and increased endothelial cell permeability.[18,35,36] In addition, maximum ESSG and magnitude of plaque topographical slope independently predict plaque erosion in humans.[17,37]

ADVERSE INFLAMMATORY OUTCOMES IN RESPONSE TO PROINFLAMMATORY ESS STIMULI. Seventeen of the 41 studied inflammatory mediators showed a statistically significant association to ESS metrics. These markers represent proinflammatory cells from the adaptive immune system and related cells from the innate immune system, as well as cytokines and chemokines implicated in atherothrombosis. The observed inflammatory relationships in response to hemodynamic stresses agree with prior descriptions of molecular participants at the culprit site of erosion.[10,11,13,14,25] However, we did observe a heterogeneity of inflammatory responses in the study population that is reflected in the marked increase of inflammatory cells (Supplemental Table 2) and cytokines (Supplemental Table 3) in the highest tertiles. These findings may reflect that some individuals had a larger plaque erosion with a greater thrombotic burden, which in turn may have resulted in a stronger inflammatory response.

Low minimum ESS and the steepness of plaque topographical slope may have synergistic effects on T-lymphocyte activation and differentiation. We found that a low minimum ESS and a steeper plaque topographical upslope were associated with an increased CL localization of T lymphocytes, including several different subsets of T lymphocytes ($CD4^+$ T lymphocytes, $CD8^+$ T lymphocytes, and NKT cells), as well as NK cells. In the published OPTICO-ACS study, eroded plaques displayed a significantly higher CR of CD4 and $CD8^+$ T lymphocytes as compared to plaques that exhibited acute rupture.[10,11] Interestingly, the T lymphocyte–related cytokine IL-2 was also increased in correlation with a steeper

plaque upslope. T lymphocytes require a high concentration of IL-2, and their differentiation depends on expression of the IL-2 receptor, as well as the strength and duration of the IL-2 signal.[38] High levels of IL-2 triggers T-lymphocyte differentiation into proinflammatory T helper 1 cells and $CD8^+$ cytotoxic T lymphocytes.[39] Recent studies also demonstrated the importance of plaque topographical slope in relation to the erosion site and found that the thrombus location, either up- or downstream of the MLA, is associated with a steeper plaque slope.[37]

The relationship of MIP-1β and shear stress is not well understood. MIP-1β has been proposed to mediate both chemotaxis and adhesion of T cells and monocytes.[40,41] We found that several adverse anatomical and biomechanical metrics associated with an increase in IL-6 and MIP-1β, supporting the notion that the pathobiologic effects of high maximum ESS result from integration of multiple adverse stimuli rather than a single independent predictor. We observed, for example, that high ESSG also associated with the same inflammatory markers, and it is unclear whether the pathobiologic effect of high ESS is only operative in the setting of an immediately adjacent low ESS (ie, high ESSG). Proinflammatory cytokine IL-6 and MIP-1β may further aggravate T-lymphocyte responses and destabilization of the plaque. In addition, IL-6 acts synergistically with IL-2 and promotes expansion and activation of T cells, in particular, $CD8^+$ T-lymphocyte differentiation into cytotoxic T cells and $CD4^+$ T-lymphocyte differentiation into T helper 1 cells.[42] Our current results support and extend previous OCT-based data correlating high ESSG as an independent biomechanical metric associated with inflammation in plaque erosion.[17,43]

INFLAMMATORY SIGNALING PATHWAY CONSEQUENCES OF LOCAL HEMODYNAMIC STRESSES. Disturbed local flow patterns with low ESS and high ESSG lead to flow-mediated activation of the nuclear factor (NF)-κB signaling pathway.[27,44] The transcription factor NF-κB is a pivotal mediator of proinflammatory responses involved in the development and progression of atherosclerotic plaques.[45] The NF-κB pathway regulates immune and inflammatory responses of both the innate and adaptive immune system involving expression of various proinflammatory genes, including those encoding cytokines and chemokines, and critically regulates the survival, activation, and differentiation of innate immune cells and inflammatory T lymphocytes.[46,47] Low shear stress has been shown to enhance human T-cell activation in vitro, including subsets of T cells $CD4^+$ and $CD8^+$ by inducing the activation of mechanosensitive ion channels that result in calcium influx and further downstream activation of the proinflammatory transcription pathway (eg, the NF-κB pathway) and consequently up-regulation of genes that encodes for proinflammatory cytokines, such as IL-1β, IL-2, and IL-6.[12,48,49] The flow-mediated activation of the NF-κB signaling pathway, based on prior in vitro studies[27] may further support a mechanistic link between low ESS, as well as high ESSG and the inflammatory signaling pathways that trigger activation, differentiation, and transmigration of T lymphocytes into the coronary plaque. Our findings add novel mechanistic insights, associating adaptive immune responses with proinflammatory biomechanical metrics previously identified as independent predictors of plaque erosions.

Prior in vitro and in vivo murine experimental atherosclerosis studies identified Toll-like receptor 2 (TLR2) as an important mediator in plaque erosion. Endothelial cells exhibit greater TLR2 expression at sites of disturbed flow. TLR2 engagement promotes endothelial cell desquamation through recruitment of neutrophils.[25,50-53] This mechanism was also demonstrated for the first time in humans in the OPTICO-ACS study, where a particular association between TLR2 and neutrophil activation in plaque erosion was established,[9] and presumably triggered by elevated soluble hyaluronic acid. This study showed a higher TLR2 expression, which prevents neutrophil apoptosis in plaque erosion/IFC-ACS, but also leads to a TLR2-mediated increase of MMP-9. This increase in MMP-9, in turn, aggravates endothelial cell detachment when combined with disturbed flow as part of the pathobiologic mechanism of plaque erosion/IFC-ACS. Ultimately TLR2 activation and signaling in endothelial cells results in sustained inflammatory responses and downstream activation of NF-κB.[54] Animal studies indicate that ESSG can regulate inflammatory responses via several mechanisms independent from the absolute value of high ESS that involve activation of endothelial TLR2 and neutrophil recruitment and accumulation.[50,53] Interestingly, we found an association between higher maximum ESSG and higher concentration of hyaluronic acid, which can be crucial for the recruitment and function of effector and memory T lymphocytes.[55] Furthermore, maximum ESSG correlates with plaque topographical slope,[37] and their immunomodulatory actions may complement each other.

In the present study a steeper plaque topographical downslope was associated with a higher CL number of neutrophils, which adds new insights to the mechanism of plaque erosion in relation to plaque

topography. However, despite neutrophils being associated with a steeper plaque downslope, we observed a significant reduction of neutrophils and granulocytes at the culprit lesion site at the time of blood sampling. This may be explained by the fact that migrated polymorphonuclear neutrophils to the site of inflammation rapidly undergo apoptosis,[56] leading to the discharge of cytokines that in turn attracts monocytes that were also found to be associated with a steeper plaque downslope. Other potential mediators of interest, not investigated in this particular study, include neutrophil enzyme myeloperoxidase that generates hypochlorous acid, a pro-oxidant implicated in endothelial injury and plaque erosion.[57]

Although we observed at the lesion site an increased concentration of granzyme A, MIP-1α, IFN-γ, MMP-9 activity, IL-8, IL-10, and IP-10, these inflammatory markers did not display an association with the biomechanical metrics under investigation. It is not yet clear whether these proinflammatory (granzyme A, MIP-1α, IFN-γ, MMP-9, IL-8) and anti-inflammatory (IP-10, IL-10) mediators are directly triggered or associated with the specific shear stress metrics under investigation. It may be that these inflammatory markers are activated further downstream in the NF-kB pathway[47] or through other signaling pathways that may not be directly triggered by the biomechanical stimuli such as the Janus kinase–signal transducer and activator of transcription (JAK-STAT)[58] signaling pathway or the c-Jun N-terminal kinase (JNK) signaling pathway.[59] Future in vitro studies will be needed to investigate why there is a local increase of granzyme A, MIP-1α, IFN-γ, MMP-9 activity, IL-8, IL-10, and IP-10 at the culprit site.

Drugs targeted to treating residual vascular inflammation offer an attractive management approach, and the mechanisms we have described may contribute to event reduction demonstrated by anti-inflammatory agents. The first human study to show promising benefit of anti-inflammatory therapy in reducing cardiovascular events, CANTOS, targeted the IL-1β innate immunity pathway with the monoclonal antibody canakinumab.[60] Colchicine, which is now approved by the US Food and Drug Administration, is the first anti-inflammatory drug indicated for reducing cardiovascular events among patients who have established atherosclerotic cardiovascular disease or are at risk of developing it.[61,62] Although the mechanistic actions of colchicine have not yet been fully established, in vivo studies have shown impaired neutrophil activation, and suppression of inflammation.[63] Mechanical amelioration of plaque topography and consequent adverse flow patterns (eg, with percutaneous coronary intervention), may also reduce local vascular inflammation in these vascular areas and thereby improve clinical outcomes.

STUDY LIMITATIONS. The study findings must be interpreted with caution. First, because the sample size was small, multiple comparisons were done, and the results were not adjusted for the multiple comparisons. Larger studies are needed to validate these findings. Second, the thrombus and blood aspiration was performed in the culprit vessel and pulled back across the entire CL, and consequently, the aspirated material may not represent solely the CL microenvironment where the thrombus originated. Although the measures of the flow dynamics and ESS are very precise with a spatial resolution of approximately 300 μm, the spatial relationship between the shear stress metrics and the extremely focal inflammatory markers may not be perfectly colocalized. In addition, the local culprit site blood sampling may have occurred many hours after the actual culprit clinical event, and the local increased concentration of inflammatory markers, initially limited to the CL site, may have "spilled over" to the systemic circulation within that time period such that a substantial concentration may have become evident both at the CL location as well as the SYS location. The biomechanical stimuli at the time of the plaque erosion may indeed have triggered a local inflammatory response and recruitment of cells from the systemic circulation to the culprit site, but it is not clear what the inflammatory patterns of bioavailability, bioactivity, or decay of these inflammatory signals are at the culprit site. Inflammatory cells may have already extravasated or undergone apoptosis to a substantial degree at the time of the blood sampling. These inflammatory relationships are most certainly highly dynamic in the setting of an ACS event. The observed association between SYS and inflammatory mediators may be owing to these uncertainties related to the blood sampling precision at the culprit site and timing of blood sample collection from the onset of the ACS event. Therefore, it will be important to develop more precise blood sampling methods that captures the detailed focal inflammatory changes at the culprit plaque site in future studies. Third, the study did not include stable "control" plaques of similar minimal and reference lumen dimensions as compared to eroded plaques to provide greater mechanistic clarity concerning the biomechanical metrics responsible for triggering the inflammatory mediators. The parent OPTICO-ACS study, however, was not designed to

include a control group, because the investigators were only interested in the local vs systemic inflammatory markers in patients with plaque rupture vs plaque erosion. Future studies will need to investigate the local and systemic inflammatory mediators with blood sampling in both plaques with erosion and stable plaques.

CONCLUSIONS

Adverse biomechanical ESS metrics associate with proinflammatory and proatherogenic cells and cytokines/chemokines and may contribute to plaque erosion. This hypothesis-generating study provides insights for future translational research directions to establish a more detailed mechanistic link between adverse ESS metrics and inflammatory responses. Overall, the results of this study reveal a complex interplay of local hemodynamic influences on inflammatory mediators and effector cells of the innate and adaptive immune response.

ACKNOWLEDGMENTS The Vascular Profiling Laboratory is grateful for the generous support of the Schaubert Family and the Macauley Family. The authors acknowledge the team of the Vascular Profiling Core Laboratory at Brigham and Women's Hospital and the collaborators at Charité University Berlin, German Centre for Cardiovascular Research, Berlin, and the Berlin Institute of Health for their contribution to the preparation of the manuscript.

FUNDING SUPPORT AND AUTHOR DISCLOSURES

Dr Libby has received funding support from the National Heart, Lung, and Blood Institute (1R01HL134892, 1R01HL163099-01, R01AG063839, R01HL151627, R01HL157073, R01HL166538), and the RRM Charitable Fund. Dr Libby is an unpaid consultant to, or involved in clinical trials for Amgen, Baim Institute, Beren Therapeutics, Esperion Therapeutics, Genentech, Kancera, Kowa Pharmaceuticals, Novo Nordisk, Novartis, and Sanofi-Regeneron. Dr Libby is a member of the scientific advisory board for Amgen, Caristo Diagnostics, CSL Behring, Eulicid Bioimaging, Kancera, Kowa Pharmaceuticals, Olatec Therapeutics, Novartis, PlaqueTec, Polygon Therapeutics, TenSixteen Bio, Soley Thereapeutics, and XBiotech, Inc. Dr Libby's laboratory has received research funding in the last 2 years from Novartis, Novo Nordisk and Genentech. Dr Libby is on the Board of Directors of XBiotech, Inc. Dr Libby has a financial interest in Xbiotech, a company developing therapeutic human antibodies, in TenSixteen Bio, a company targeting somatic mosaicism and clonal hematopoiesis of indeterminate potential (CHIP) to discover and develop novel therapeutics to treat age-related diseases, and in Soley Therapeutics, a biotechnology company that is combining artificial intelligence with molecular and cellular response detection for discovering and developing new drugs, currently focusing on cancer therapeutics. Dr Libby's interests were reviewed and are managed by Brigham and Women's Hospital and Mass General Brigham in accordance with their conflict-of-interest policies. Dr Landmesser has received institutional research grants from Amgen, Abbott, Bayer and Novartis. Dr Abdelwahed receives consultancy fees from Boston Scientific and Shockwave. Dr Stone's laboratory was funded by the National Heart, Lung, and Blood Institute (R01HL146144-01A1 and R01HL140498). Dr Ahmed was supported by grants from the Swedish Heart-Lung Foundation (20200165 and 20230167), the Swedish Research Council (202100456), the Swedish Society of Medicine (SLS-961835), Erik and Edith Fernströms Foundation (FS-2021:0004), Karolinska Institutet (FS2020:0007), the Sweden-America Foundation, and the Swedish Heart Foundation. All other authors have reported that they have no relationships relevant to the contents of this paper to disclose.

ADDRESS FOR CORRESPONDENCE: Dr Peter H. Stone, Division of Cardiovascular Medicine, Brigham and Women's Hospital, 75 Francis Street, Boston, Massachusetts 02115, USA. E-mail: pstone@bwh.harvard.edu.

PERSPECTIVES

COMPETENCY IN MEDICAL KNOWLEDGE: Plaque erosion has distinct clinical, pathobiological, and molecular characteristics from ruptured fibrous plaque. It is essential to understand the underlying biomechanical and molecular mechanisms that trigger plaque erosion and thrombus formation to enable early identification, and possible pre-emptive intervention, of such high-risk plaques before they destabilize. Our findings raise interesting and clinically important vascular biology questions that reach beyond ACS, such as how local coronary arterial interventions (eg, coronary stent deployment) may alter the regional shear stress environment in ways that influence healing vs thrombosis and vascular inflammation. Greater understanding of the underlying mechanisms of plaque erosion may inform the development of novel biomarkers and drug therapies and guide tailored treatments of patients with, or at risk of, an ACS.

TRANSLATIONAL OUTLOOK: These findings highlight the need for further studies to explore the links between adverse biomechanical stimuli and the regulation of proinflammatory mediators and their participation in coronary plaque erosion. Other biomechanical stimuli may also be involved in the processes of inflammatory pathway activation and creation of other pathobiological phenotypes of plaque destabilization through a variety of mechanisms, acting either alone or in combination.

REFERENCES

1. Khan MA, Hashim MJ, Mustafa H, et al. Global epidemiology of ischemic heart disease: results from the Global Burden of Disease Study. *Cureus*. 2020;12(7):e9349.

2. Virmani R, Kolodgie FD, Burke AP, Farb A, Schwartz SM. Lessons from sudden coronary death: a comprehensive morphological classification scheme for atherosclerotic lesions. *Arterioscler Thromb Vasc Biol*. 2000;20(5):1262–1275.

3. Libby P. Mechanisms of acute coronary syndromes. *N Engl J Med*. 2013;369(9):883–884.

4. Partida RA, Libby P, Crea F, Jang IK. Plaque erosion: a new in vivo diagnosis and a potential major shift in the management of patients with acute coronary syndromes. *Eur Heart J*. 2018;39(22):2070–2076.

5. Saia F, Komukai K, Capodanno D, et al. Eroded versus ruptured plaques at the culprit site of STEMI: in vivo pathophysiological features and response to primary PCI. *JACC Cardiovasc Imaging*. 2015;8(5):566–575.

6. van der Wal AC, Becker AE, van der Loos CM, Das PK. Site of initial rupture or erosion of thrombosed coronary atherosclerotic plaques is characterized by an inflammatory process irrespective of the dominant plaque morphology. *Circulation*. 1994;89(1):36–44.

7. Chandran S, Watkins J, Abdul-Aziz A, et al. Inflammatory differences in plaque erosion and rupture in patients with ST-segment elevation myocardial infarction. *J Am Heart Assoc*. 2017;6(5):e005868.

8. Gerhardt T, Seppelt C, Abdelwahed YS, et al. Culprit plaque morphology determines inflammatory risk and clinical outcomes in acute coronary syndrome. *Eur Heart J*. 2023;44(38):3911–3925.

9. Meteva D, Vinci R, Seppelt C, et al. Toll-like receptor 2, hyaluronan, and neutrophils play a key role in plaque erosion: the OPTICO-ACS study. *Eur Heart J*. 2023;44(38):3892–3907.

10. Leistner DM, Krankel N, Meteva D, et al. Differential immunological signature at the culprit site distinguishes acute coronary syndrome with intact from acute coronary syndrome with ruptured fibrous cap: results from the prospective translational OPTICO-ACS study. *Eur Heart J*. 2020;41(37):3549–3560.

11. Libby P. Inflammation during the life cycle of the atherosclerotic plaque. *Cardiovasc Res*. 2021;117(13):2525–2536.

12. Chatzizisis YS, Coskun AU, Jonas M, Edelman ER, Feldman CL, Stone PH. Role of endothelial shear stress in the natural history of coronary atherosclerosis and vascular remodeling: molecular, cellular, and vascular behavior. *J Am Coll Cardiol*. 2007;49(25):2379–2393.

13. Gregory F. Role of mechanical stress and neutrophils in the pathogenesis of plaque erosion. *Atherosclerosis*. 2021;318:60–69.

14. Quillard T, Franck G, Mawson T, Folco E, Libby P. Mechanisms of erosion of atherosclerotic plaques. *Curr Opin Lipidol*. 2017;28(5):434–441.

15. Stone PH, Maehara A, Coskun AU, et al. Role of low endothelial shear stress and plaque characteristics in the prediction of nonculprit major adverse cardiac events: the PROSPECT study. *JACC Cardiovasc Imaging*. 2018;11(3):462–471.

16. Stone PH, Saito S, Takahashi S, et al. Prediction of progression of coronary artery disease and clinical outcomes using vascular profiling of endothelial shear stress and arterial plaque characteristics: the PREDICTION study. *Circulation*. 2012;126(2):172–181.

17. Thondapu V, Mamon C, Poon EKW, et al. High spatial endothelial shear stress gradient independently predicts site of acute coronary plaque rupture and erosion. *Cardiovasc Res*. 2021;117(8):1974–1985.

18. LaMack JA, Himburg HA, Li XM, Friedman MH. Interaction of wall shear stress magnitude and gradient in the prediction of arterial macromolecular permeability. *Ann Biomed Eng*. 2005;33(4):457–464.

19. Cochain C, Zernecke A. Protective and pathogenic roles of CD8(+) T cells in atherosclerosis. *Basic Res Cardiol*. 2016;111(6):71.

20. Grivel JC, Ivanova O, Pinegina N, et al. Activation of T lymphocytes in atherosclerotic plaques. *Arterioscler Thromb Vasc Biol*. 2011;31(12):2929–2937.

21. Tearney GJ, Regar E, Akasaka T, et al. Consensus standards for acquisition, measurement, and reporting of intravascular optical coherence tomography studies: a report from the International Working Group for Intravascular Optical Coherence Tomography Standardization and Validation. *J Am Coll Cardiol*. 2012;59(12):1058–1072.

22. Jia H, Abtahian F, Aguirre AD, et al. In vivo diagnosis of plaque erosion and calcified nodule in patients with acute coronary syndrome by intravascular optical coherence tomography. *J Am Coll Cardiol*. 2013;62(19):1748–1758.

23. Coskun AU, Yeghiazarians Y, Kinlay S, et al. Reproducibility of coronary lumen, plaque, and vessel wall reconstruction and of endothelial shear stress measurements in vivo in humans. *Catheter Cardiovasc Interv*. 2003;60(1):67–78.

24. Gijsen F, Katagiri Y, Barlis P, et al. Expert recommendations on the assessment of wall shear stress in human coronary arteries: existing methodologies, technical considerations, and clinical applications. *Eur Heart J*. 2019;40(41):3421–3433.

25. Fahed AC, Jang IK. Plaque erosion and acute coronary syndromes: phenotype, molecular characteristics and future directions. *Nat Rev Cardiol*. 2021;18(10):724–734.

26. Davies PF, Remuzzi A, Gordon EJ, Dewey CF Jr, Gimbrone MA Jr. Turbulent fluid shear stress induces vascular endothelial cell turnover in vitro. *Proc Natl Acad Sci U S A*. 1986;83(7):2114–2117.

27. Nagel T, Resnick N, Dewey CF Jr, Gimbrone MA Jr. Vascular endothelial cells respond to spatial gradients in fluid shear stress by enhanced activation of transcription factors. *Arterioscler Thromb Vasc Biol*. 1999;19(8):1825–1834.

28. Zhao Y, Ren P, Li Q, et al. Low shear stress upregulates CX3CR1 expression by inducing VCAM-1 via the NF-kappaB pathway in vascular endothelial cells. *Cell Biochem Biophys*. 2020;78(3):383–389.

29. Yamamoto E, Siasos G, Zaromytidou M, et al. Low endothelial shear stress predicts evolution to high-risk coronary plaque phenotype in the future: a serial optical coherence tomography and computational fluid dynamics study. *Circ Cardiovasc Interv*. 2017;10(8):e005455.

30. Korshunov VA, Berk BC. Strain-dependent vascular remodeling: the "Glagov phenomenon" is genetically determined. *Circulation*. 2004;110(2):220–226.

31. Brown AJ, Teng Z, Evans PC, Gillard JH, Samady H, Bennett MR. Role of biomechanical forces in the natural history of coronary atherosclerosis. *Nat Rev Cardiol*. 2016;13(4):210–220.

32. McElroy M, Kim Y, Niccoli G, et al. Identification of the haemodynamic environment permissive for plaque erosion. *Sci Rep*. 2021;11(1):7253.

33. Samady H, Eshtehardi P, McDaniel MC, et al. Coronary artery wall shear stress is associated with progression and transformation of atherosclerotic plaque and arterial remodeling in patients with coronary artery disease. *Circulation*. 2011;124(7):779–788.

34. Dolan JM, Meng H, Sim FJ, Kolega J. Differential gene expression by endothelial cells under positive and negative streamwise gradients of high wall shear stress. *Am J Physiol Cell Physiol*. 2013;305(8):C854–C866.

35. DePaola N, Gimbrone MA Jr, Davies PF, Dewey CF Jr. Vascular endothelium responds to fluid shear stress gradients. *Arterioscler Thromb*. 1992;12(11):1254–1257.

36. Tardy Y, Resnick N, Nagel T, Gimbrone MA Jr, Dewey CF Jr. Shear stress gradients remodel endothelial monolayers in vitro via a cell proliferation-migration-loss cycle. *Arterioscler Thromb Vasc Biol*. 1997;17(11):3102–3106.

37. Hakim D, Pinilla-Echeverri N, Coskun AU, et al. The role of endothelial shear stress, shear stress gradient, and plaque topography in plaque erosion. *Atherosclerosis*. 2023;376:11–18.

38. Glassman CR, Su L, Majri-Morrison SS, et al. Calibration of cell-intrinsic interleukin-2 response thresholds guides design of a regulatory T cell biased agonist. *Elife*. 2021;10:e65777.

39. Ross SH, Cantrell DA. Signaling and function of interleukin-2 in T lymphocytes. *Annu Rev Immunol*. 2018;36:411–433.

40. Tanaka Y, Adams DH, Hubscher S, Hirano H, Siebenlist U, Shaw S. T-cell adhesion induced by proteoglycan-immobilized cytokine MIP-1 beta. *Nature*. 1993;361(6407):79–82.

41. Tatara Y, Ohishi M, Yamamoto K, et al. Macrophage inflammatory protein-1beta induced cell adhesion with increased intracellular reactive

oxygen species. *J Mol Cell Cardiol*. 2009;47(1):104–111.

42. Reiss AB, Siegart NM, De Leon J. Interleukin-6 in atherosclerosis: atherogenic or atheroprotective? *Clin Lipid*. 2017;12(1):14–23.

43. Yamamoto E, Thondapu V, Poon E, et al. Endothelial shear stress and plaque erosion: a computational fluid dynamics and optical coherence tomography study. *JACC Cardiovasc Imaging*. 2019;12(2):374–375.

44. Baeriswyl DC, Prionisti I, Peach T, et al. Disturbed flow induces a sustained, stochastic NF-kappaB activation which may support intracranial aneurysm growth in vivo. *Sci Rep*. 2019;9(1):4738.

45. Hajra L, Evans AI, Chen M, Hyduk SJ, Collins T, Cybulsky MI. The NF-kappa B signal transduction pathway in aortic endothelial cells is primed for activation in regions predisposed to atherosclerotic lesion formation. *Proc Natl Acad Sci U S A*. 2000;97(16):9052–9057.

46. Lawrence T. The nuclear factor NF-kappaB pathway in inflammation. *Cold Spring Harb Perspect Biol*. 2009;1(6):a001651.

47. Liu T, Zhang L, Joo D, Sun SC. NF-kappaB signaling in inflammation. *Signal Transduct Target Ther*. 2017;2:17023.

48. Gimbrone MA Jr, Topper JN, Nagel T, Anderson KR, Garcia-Cardena G. Endothelial dysfunction, hemodynamic forces, and atherogenesis. *Ann N Y Acad Sci*. 2000;902:230–239. discussion 239-240.

49. Hope JM, Dombroski JA, Pereles RS, et al. Fluid shear stress enhances T cell activation through Piezo1. *BMC Biol*. 2022;20(1):61.

50. Franck G, Mawson T, Sausen G, et al. Flow perturbation mediates neutrophil recruitment and potentiates endothelial injury via TLR2 in mice: implications for superficial erosion. *Circ Res*. 2017;121(1):31–42.

51. Giannotta M, Trani M, Dejana E. VE-cadherin and endothelial adherens junctions: active guardians of vascular integrity. *Dev Cell*. 2013;26(5):441–454.

52. Mullick AE, Soldau K, Kiosses WB, Bell TA 3rd, Tobias PS, Curtiss LK. Increased endothelial expression of Toll-like receptor 2 at sites of disturbed blood flow exacerbates early atherogenic events. *J Exp Med*. 2008;205(2):373–383.

53. Quillard T, Araujo HA, Franck G, Shvartz E, Sukhova G, Libby P. TLR2 and neutrophils potentiate endothelial stress, apoptosis and detachment: implications for superficial erosion. *Eur Heart J*. 2015;36(22):1394–1404.

54. Oliveira-Nascimento L, Massari P, Wetzler LM. The role of TLR2 in infection and immunity. *Front Immunol*. 2012;3:79.

55. Baaten B, Tinoco R, Chen A, Bradley L. Regulation of antigen-experienced T cells: lessons from the quintessential memory marker CD44. *Immunol*. 2012;27(3):23.

56. Soehnlein O, Lindbom L, Weber C. Mechanisms underlying neutrophil- mediated monocyte recruitment. *Blood*. 2009;114(21):4613–4623.

57. Sugiyama S, Kugiyama K, Aikawa M, Nakamura S, Ogawa H, Libby P. Hypochlorous acid, a macrophage product, induces endothelial apoptosis and tissue factor expression: involvement of myeloperoxidase-mediated oxidant in plaque erosion and thrombogenesis. *Arterioscler Thromb Vasc Biol*. 2004;24(7):1309–1314.

58. Banerjee S, Biehl A, Gadina M, Hasni S, Schwartz DM. JAK-STAT signaling as a target for inflammatory and autoimmune diseases: current and future prospects. *Drugs*. 2017;77(5):521–546.

59. Liu Q, Pan J, Bao L, et al. Major vault protein prevents atherosclerotic plaque destabilization by suppressing macrophage ASK1-JNK signaling. *Arterioscler Thromb Vasc Biol*. 2022;42(5):580–596.

60. Ridker PM, Everett BM, Thuren T, et al. Antiinflammatory therapy with canakinumab for atherosclerotic disease. *N Engl J Med*. 2017;377(12):1119–1131.

61. Opstal TSJ, Nidorf SM, Fiolet ATL, et al. Drivers of mortality in patients with chronic coronary disease in the low-dose colchicine 2 trial. *Int J Cardiol*. 2023;372:1–5.

62. Nidorf SM, Fiolet ATL, Mosterd A, et al. Colchicine in patients with chronic coronary disease. *N Engl J Med*. 2020;383(19):1838–1847.

63. Lockhart SM, O'Rahilly S. Colchicine-an old dog with new tricks. *Nat Metab*. 2021;3(4):451–452.

KEY WORDS coronary atherosclerosis, endothelial shear stress, inflammation, plaque erosion

APPENDIX For supplemental methods, tables, and references, please see the online version of this paper.